Supporting Information

Ultrahigh Nitrogen-Doped Hollow Carbon Spheres with Hierarchical Pores for High-Reversibility Lithium-Sulfur Batteries

Qingkai Zeng, Xiaolan Li, Jinliang Zhu, Guifang Wang, Xiyong Chen, Shaojian Ma and Pei Kang Shen*

Guangxi Key Laboratory of Processing for Non-ferrous Metals and Featured Materials, School of Resources, Environment and Materials, Collaborative Innovation Center of Sustainable Energy Materials, Guangxi University, 100 Daxue Dong Road, Nanning 530004, PR China.

*Corresponding authors: Email: jlzhu85@163.com (Jinliang Zhu)

Experimental Section

Preparation of NHCS-x/S, x = 1-3.

Silica particles (size: 20 nm, 1.5 g), melamine (14 g), and formaldehyde (10 g) were added to 200 mL of water under stirring. The suspension was heated to 60 °C and stirred for 3 h, adjusted to pH = 3, stirred for another 1 h, and then cooled to room temperature to obtain a white precipitate. After centrifugation, the precipitate was dried at 100 °C for 1 h to obtain nano-silica coated with melamine-formaldehyde resin. Carbonization at 800 °C for 2 h in an argon atmosphere produced the nano-silica coated with carbon microspheres. Then, the silica core was removed by soaking in 1000 mL of 10% HF aqueous solution for 5 h. After separation by centrifugation, the final product was washed with deionized water to pH neutral and dried. These ultrahigh nitrogen-doped hollow carbon spheres with hierarchical pores were labeled NHCS-1. NHCS-2 and NHCS-3 were prepared similarly, except that the carbonization temperature was 1000 °C and 1200 °C, respectively. The sulfur electrode materials (NHCS-x/S, x = 1-3) were typically prepared by manually mixing NHCS-x and S in a weight ratio of 1:3 and then heating the mixture at 155 °C for 12 h**.**

Physical characterization.

XRD patterns were collected using a D/Max-III X-ray diffractometer (Rigaku Co., Japan) with Cu Kα radiation, and the voltage and current were 40 kV and 30 mA, respectively. A Raman spectrometer (Horiba Jobin Yvon Inc., France) using a 532-nm He/Ne laser was used to obtain the Raman spectra. The specific surface area and pore size distribution were analyzed using an ASAP 2460 surface area analyzer (Micromeritics Co., USA). The S content was measured using a thermogravimetric analyzer (DSC/TGA; Netzsch STA449 F5 Jupiter) under N_2 from 30 to 850 °C. The conductivity of samples were analyzed by ST-2722 semiconductor resistivity of the powder tester (Suzhou Jingge Electronic Co., Ltd). UV-vis adsorption spectra were measured using an

ultraviolet/visible spectrophotometer (PerkinElmer Lambda650, USA). To characterize the surface composition and chemical state of the samples, X-ray photoelectron spectroscopy (XPS) analysis was performed using an ESCALAB 250 spectrometer with a single-color Al Kα radiation source. Field-emission scanning electron microscopy (SEM, SU8820, Hitachi Co., Japan) and transmission electron microscopy (TEM, Titan ETEM G2, USA) were used to analyze the morphology and elemental distribution of the materials.

Visual observation of polysulfide adsorption.

A Li_2S_6 solution (5 mmol/L) was prepared by adding a mixture of sulfur and lithium sulfide (molar ratio: 1:5) to a mixed solvent of 1,2-dimethoxyethane/1,3-dioxolane (DME/DOL, 1:1 v/v), followed by stirring for 24 h at 60 °C. To visually observe the polysulfide adsorption, 20 mg of the carbon host was added to 4 mL Li_2S_6 solution, and photographs were taken after 15h at room temperature. An ultraviolet/visible spectrophotometer was used to investigate the adsorption capacity of the three carbon hosts.

Symmetric cells for cyclic voltammetry analysis.

To prepare electrodes for the symmetric cells, NHCS-1, NHCS-2, or NHCS-3 was homogeneously mixed with acetylene black and polyvinylidene fluoride (PVDF) at 7:2:1 mass ratio in N-methyl-2-pyrrolidinone (NMP) to form a slurry, which was coated on an aluminum foil with a loading of 0.5 mg cm^{-2}. Two identical electrodes were assembled into a 2032coin cell, and Li_2S_6 in DOL/DME (0.2 M, 50.0μL) was used as the active species. The cyclic voltammetry (CV) curves were obtained in the voltage range from -0.8 to 0.8 V with a scan rate of 20 mV s^{-1}. The frequency range of the electrochemical impedance spectroscopy (EIS) tests was 100 kHz to 10 mHz using

5mV as a voltage amplitude. Both CV and EIS experiments were carried out on an IM6 electrochemical workstation (Zahner-Elektrik, Germany).

Nucleation of Li_2S

Li_2S and S (1:7 molar ratio) were dissolved in a mixed solvent of DOL/DME (1:1 v/v) containing 1.0 M lithium bis(trifluoromethanesulfonyl)imide (LiTFSI), followed by vigorous stirring at 80 °C to prepare the Li_2S_8 electrolyte. The NHCS sample was suspended in ethanol and added dropwise to a piece of carbon cloth (diameter: 14 mm). After drying at 60 °C for 12 h, the working electrode was obtained. The nucleation of Li_2S was examined in a 2032 coin cell with a Li foil as the counter electrode, Celgard 2400 separator, and NHCS/carbon cloth as the working electrode. The Li_2S_8 catholyte (30 μL) was dropped onto the counter working electrode, and 30 μL of blank electrolyte with 1wt% $LiNO_3$ and no Li_2S_8 was added to the counter electrode. The cells were discharged galvanostatically at 0.112 mA to 2.11 V and kept potentiostatically at 2.10 V with a battery testing system (Shenzhen Neware Battery Co).

Density functional theory calculation

First-principles calculations were performed within the framework of density functional theory (DFT) using the projector-augmented plane-wave method. The Perdew-Burke-Ernzerhof type gradient-corrected exchange-correlation potential was employed. A cutoff energy of 500 eV was used for the plane wave basis set, and a vacuum layer of 15 Å was set along the Z direction to avoid interactions between periodic images. All atoms were allowed to completely relax until the force on each was less than 0.01 eV/Å. The DFT-D3 method was used to describe dispersion interactions. The interaction energy between the adsorbate and substrate was calculated as $\Delta E = E_{sub/ad} - E_{ad} - E_{sub}$,

where $E_{sub/ad}$ represents the energy of the whole absorption system, E_{ad} is that of the adsorbate, and E_{sub} is that of the substrate.

Electrochemical measurements

To prepare the cathode, a homogeneous slurry was prepared by mixing 70 wt% NHCS-x(x=1,2,3), 20 wt% acetylene black, and 10 wt% PVDF in NMP. The slurry was spread on an aluminum foil (diameter: 14 mm) and dried at 50 °C overnight with a sulfur loading of 1.2 mg cm^{-2}. Half cells of the 2032 coin type were fabricated using the NHCS-x/S composite as cathode and Li metal as counter electrode. The electrolyte contained 1.0 M LiTFSI and 1 wt% $LiNO_3$ as additive in DOL+DME (1:1, v/v). The electrochemical performances were measured on a battery testing system (Shenzhen Neware Battery Co., China) at 1.7-2.8 V. CV tests were carried out on a IM6 electrochemical workstation (Zahner-Elektrik, Germany) in the potential range of 1.7-2.8 V with a rate of 0.1 mV s^{-1}. EIS analysis was performed in a frequency range from 100 kHz to 10 mHz using 5mV as a voltage amplitude.

In situ Raman spectroscopy and in situ XRD measurements

A Li-S battery equipped with a quartz window (Beijing Scistar Technology Co. Ltd., China) was used to record the *in situ* Raman spectra in the wavenumber range of 50-600 cm^{-1}. While the battery was charged and discharged at a current density of 0.2C, Raman data were collected in steps of 0.1 V. The in situ XRD experiments used a polyimide film (Beijing Scistar Technology Co., Ltd.). The diffraction patterns were recorded in the 2θ of 22-30° every 0.1 V while the battery was charged and discharged at a current density of 0.2 C.

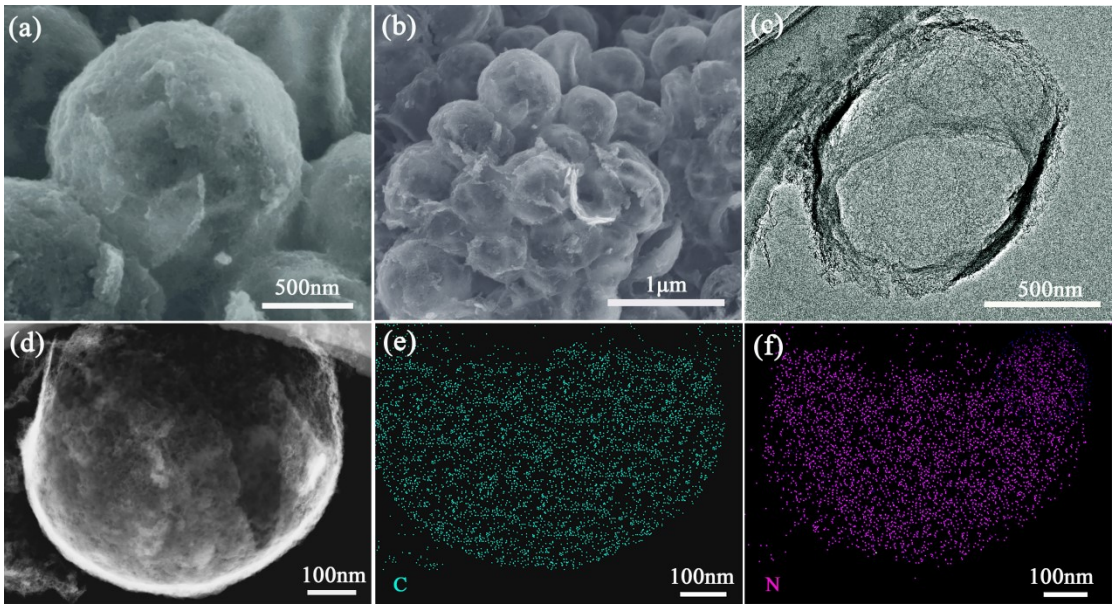

Fig. S1 (a-b) SEM images of NHCS-1. (c) TEM and (d)STEM images of NHCS-1. (e-f) elemental mappings of NHCS-1.

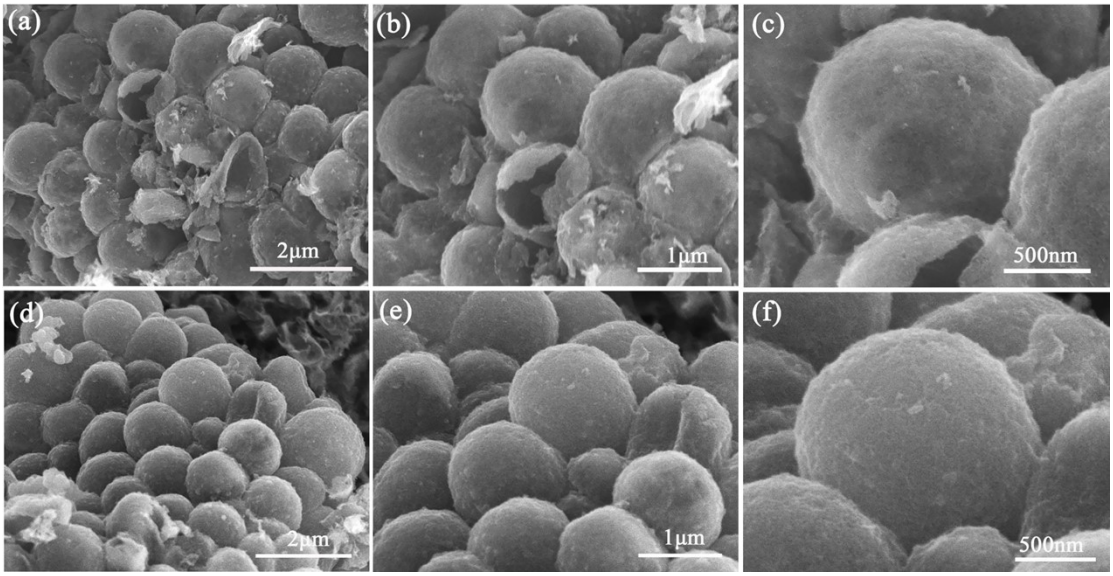

Fig. S2 (a-c) SEM images of NHCS-2. (d-f) SEM images of NHCS-3.

Table S1. Nitrogen content and different nitrogen composition of NHCS samples.

	N content	Pyridinic N	Pyrrolic N	Graphitic N
NHCS-1	18.94 at%	8.71 at%	9.49 at%	0.74 at%
NHCS-2	7.87 at%	2.48 at%	4.00 at%	1.39 at%
NHCS-3	3.08 at%	0.50 at%	2.06 at%	0.52 at%

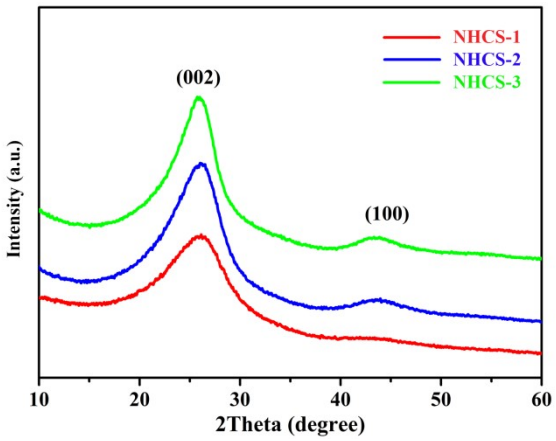

Fig. S3 XRD patterns of NHCS-1, NHCS-2 and NHCS-3

Fig. S4 (a-c) Conductivity of NHCS-1, NHCS-2 and NHCS-3

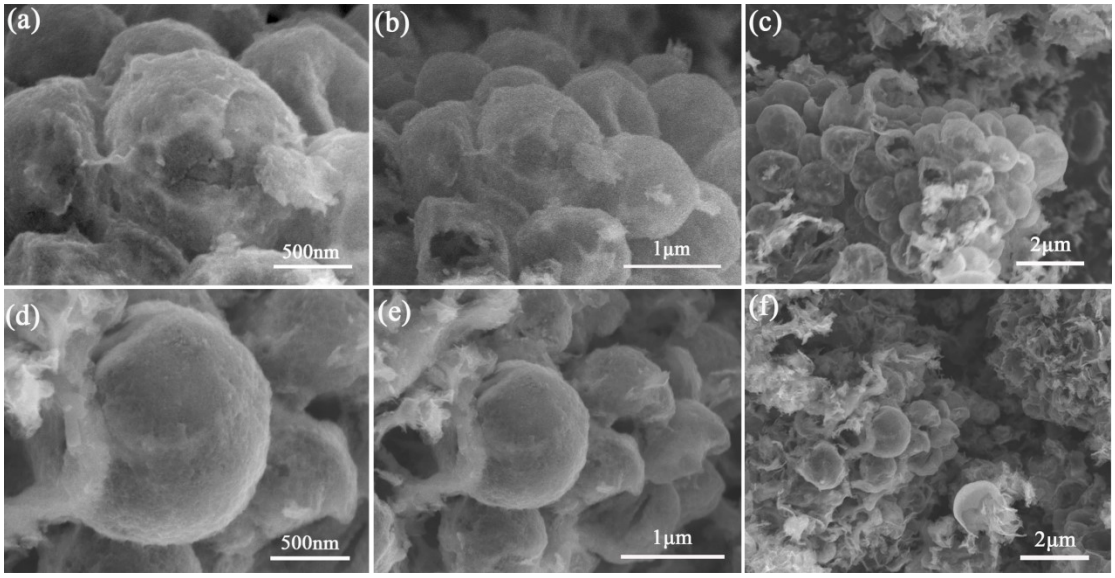

Fig. S5 (a-c) SEM images of NHCS-2/S. (d-f) SEM images of NHCS-3/S

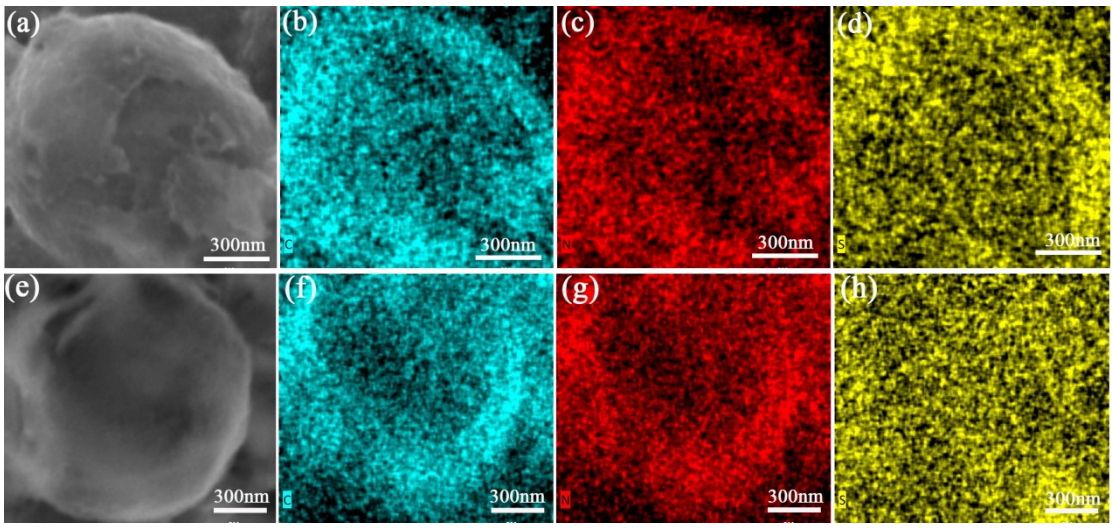

Fig. S6 (a-d) Elemental mapping images of NHCS-2/S. (e-f) Elemental mapping images of NHCS-3/S.

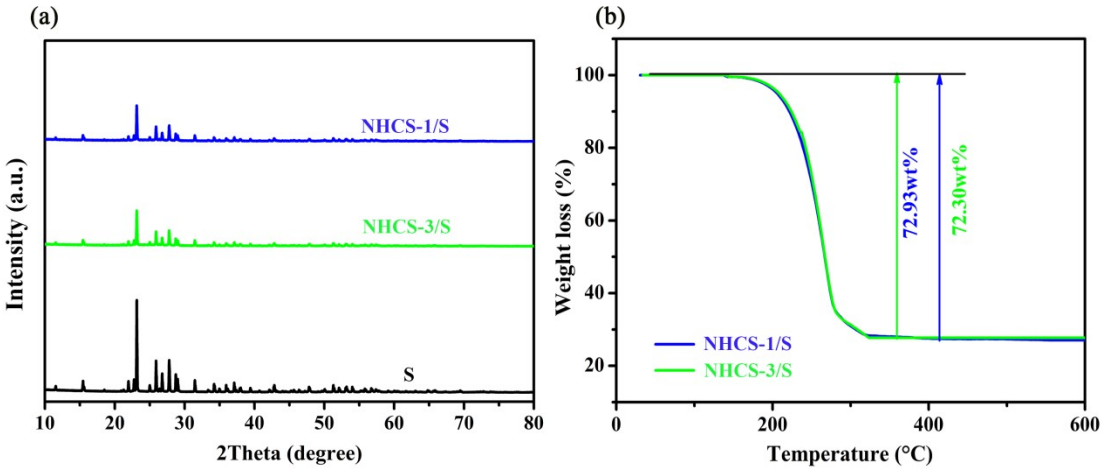

Fig. S7 (a) XRD patterns of NHCS-2/S, NHCS-3/S and (b) TG curves of NHCS-2/S and NHCS-3/S.

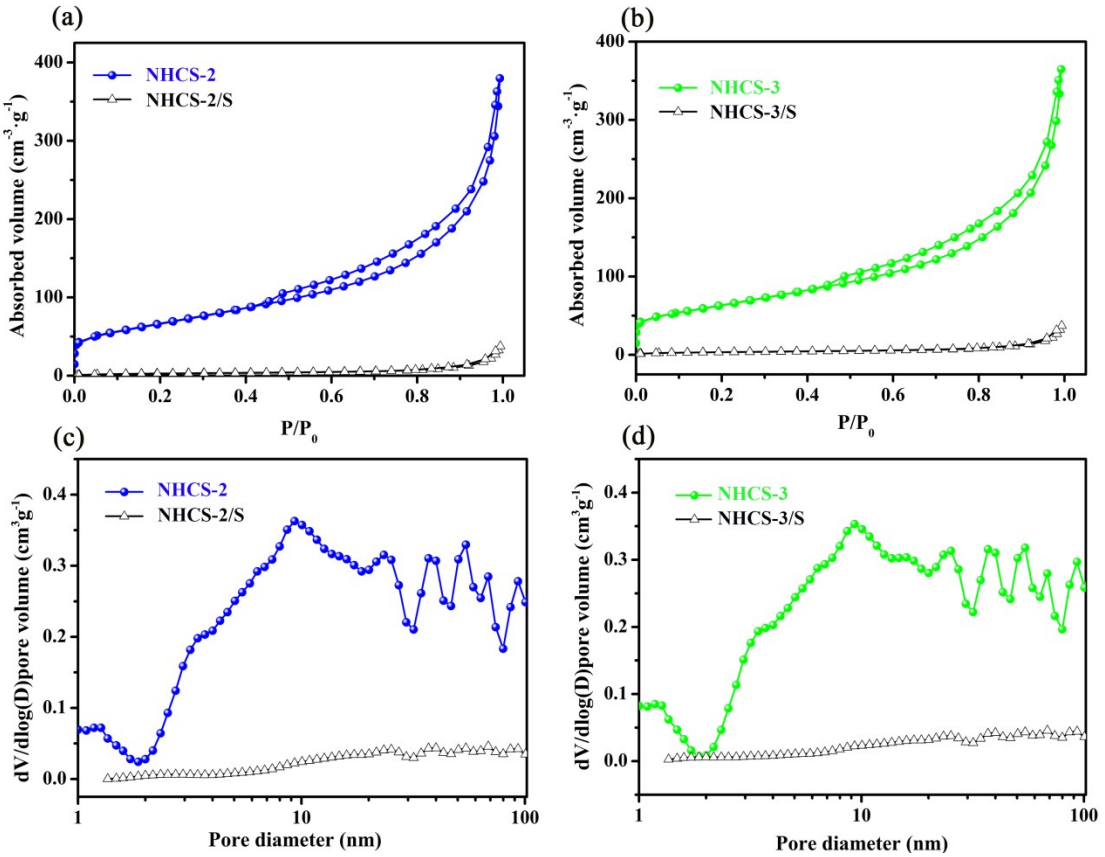

Fig. S8 (a) N_2 adsorption-desorption isotherms of NHCS-2 and NHCS-2/S and (b) N_2 adsorption-desorption isotherms of NHCS-3 and NHCS-3/S. (c) pore size distributions of NHCS-2 and NHCS-2/S and (d) pore size distributions of NHCS-3 and NHCS-3/S.

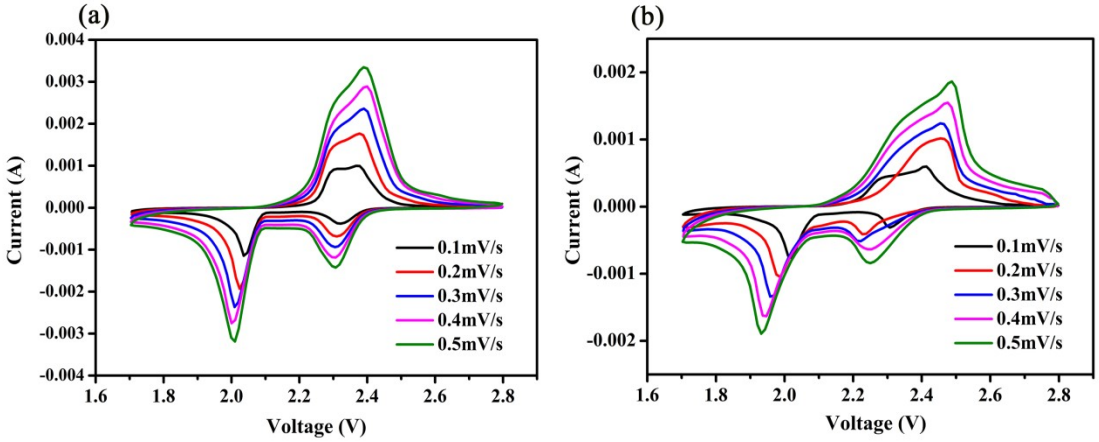

Fig. S9 CV curves of (a)NHCS-2/S and (b) NHCS-3/S at different scan rates

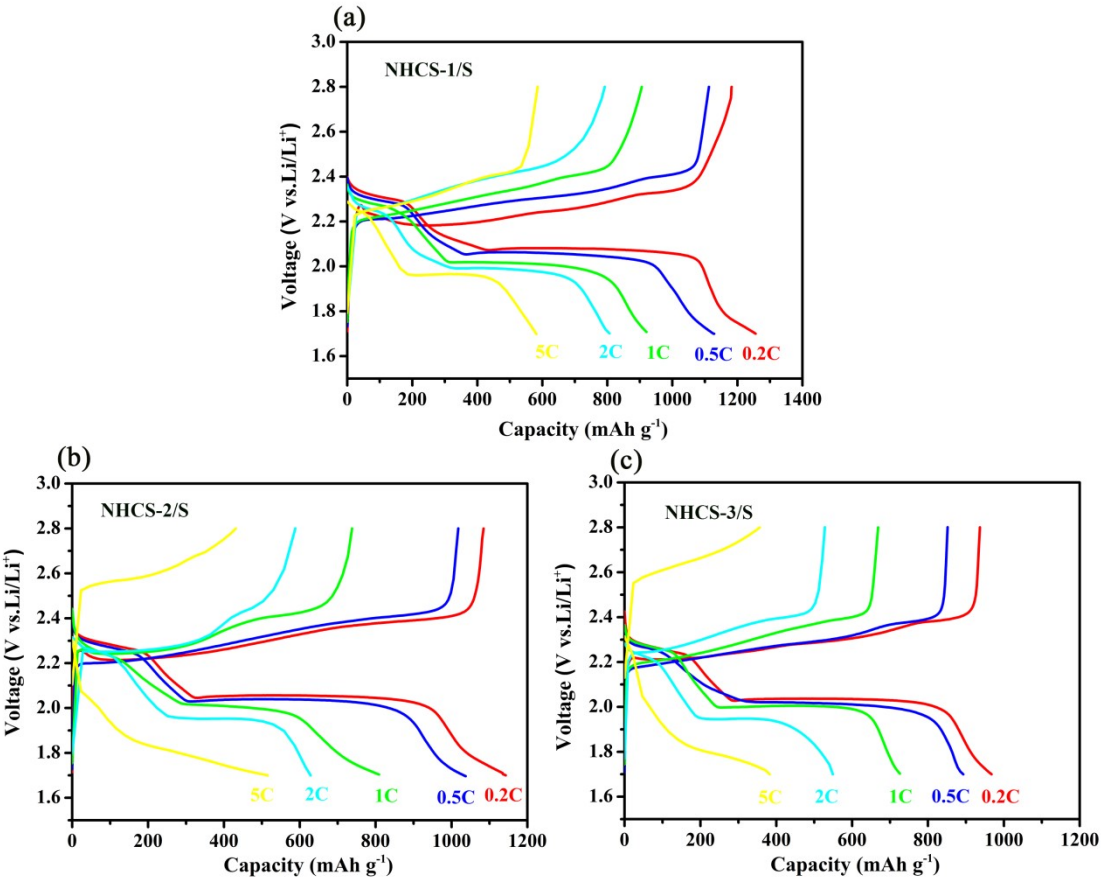

Fig. S10 Charge-discharge profiles at different current density of NHCS-1/S, NHCS-2/S and NHCS-3/S.

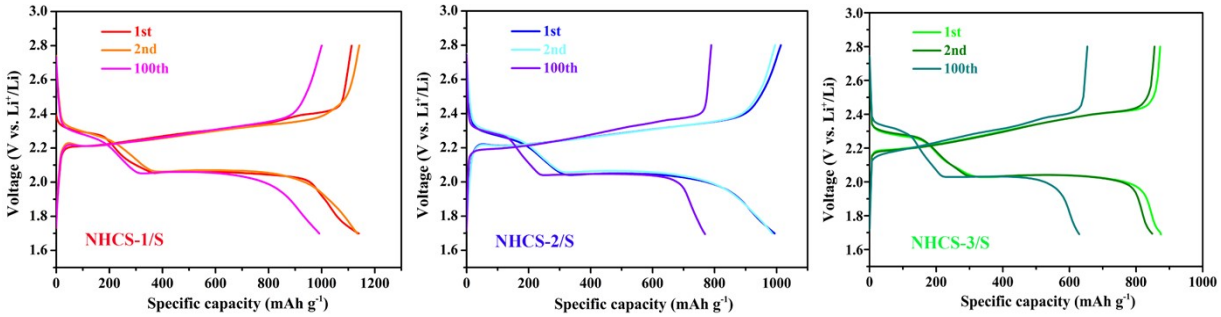

Fig. S11 Charge-discharge profiles of NHCS-1/S, NHCS-2/S and NHCS-3/S for the 1st, 2nd, and 100th cycles at 0.5C.

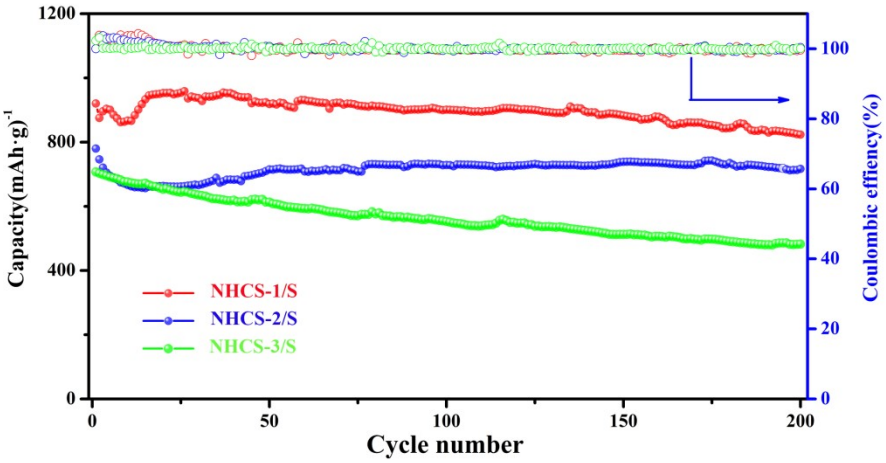

Fig. S12 Long-term cycling performance of NHCS-1/S, NHCS-2/S and NHCS-3/S for 200 cycles at the current density of 1C.

Table S2. Initial capacity, capacity after cycling and capacity retention of NHCS-1/S, NHCS-2/S and NHCS-3/S.

Sample	Initial capacity (mAh g^{-1})	Capacity after cycling (mAh g^{-1})	Capacity retention (%)
NHCS-1/S	920.33	823.56	89.48
NHCS-2/S	780.13	713.32	91.43
NHCS-3/S	707.49	479.17	67.73

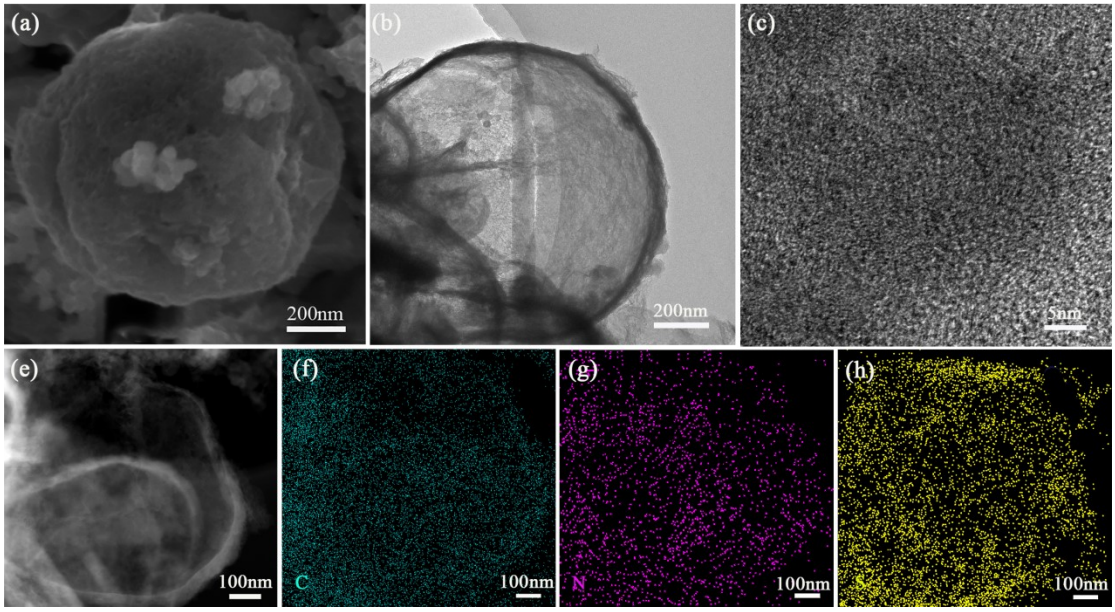

Fig. S13 (a) SEM image of NHCS-1/S after cycling tests. (b) TEM images of NHCS-1/S after cycling tests. (c) HRTEM image of NHCS-1/S after cycling test. (e-g) Elemental mappings of NHCS-1/S after cycling test.

Table S3. Comparison of NHCS-1/S with carbon materials recently reported in literatures for Li-S batteries

	Sulfur content	C-rate	Cycle number	Initial capacity (mAh g^{-1})	Reversible capacity (mAh g^{-1})	Capacity decay rate per cycle	High-rate-Capability (mAg h^{-1})	Ref.
NHCS-1/S	71.8%	0.5C 1C 2C	100 200 500	1138.6 920.3 806.5	991.3 823.6 691.3	0.129% 0.05% 0.028%	804.9 (2C) 637.1 (5C)	This work
BOC@CNT/S	72.4%	1C	500	1210	794	0.07%	768 (2C) 636 (5C)	S1
P@E-CNTs/S	72%	0.5C	200	992	735	0.129%	562 (2C) 462 (3C)	S2
N-HC/S	64.3%	1C	1000	721.8	360.9	0.05%	467.4 (2C) 208.3 (3C)	S3
MHCSs/S	73%	1C	500	1196	630	0.158%	715 (2C) 592 (5C)	S4
NPDSCS-S	72.4%	0.5C 1C	100 500	1106 952	975 814	0.116% 0.029%	826 (2C) 697 (3C)	S5
CF@G/S	78%	0.5C 1C	1000 1000	1203.2 1016.8	721.9 508.4	0.04% 0.05%	464.6 (2C)	S6
S/PCMSs/S	70%	0.5C	700	932	489	0.067%	830 (2C) 780 (3C) 742 (4C)	S7
3DCNF/S	60%	0.5C 1C	500 300	977 800	607 544	0.07% 0.106%	-	S8
G-HPC/S	67.5%	0.5C	100	854.0	792.6	0.071%	761.4 (1C) 433.6 (2C)	S9
NCNTs-CS/S	70%	1C	700	889	564	0.052 %	618 (2C)	S10
PGC@HEWC/S	57.5%	1C	400	921	795	0.034%	817 (2C)	S11
HNPC-S	65%	0.5C 2C	400	1010 785	788 562	0.055% 0.032%	781(2C) 623 (5C)	S12

References

[S1] X. Chen, Y. Xu, F. H. Du, Y. Wang, *Small Methods*, 2019, **3**, 1900338.

[S2] M. Yan, H. Chen, Y. Yu, H. Zhao, C. F. Li, Z. Y. Hu, P. Wu, L. Chen, H. Wang, D. Peng, H. Gao, T. Hasan, Y. Li, B. L. Su, *Adv. Energy Mater*., 2018, **8**, 1801066.

[S3] J. S. Yeon, S. H. Park, J. Suk, H. Lee, H. S. Park, *Chem. Eng. J*., 2020, **382**, 122946.

[S4] M. Chen, Z. Su, K. Jiang, Y. Pan, Y. Zhang, D. Long, *J. Mater. Chem. A*, 2019, **7**, 6250-6258.

[S5] J. Wang, H. Yang, Z. Chen, L. Zhang, J. Liu, P. Liang, H. Yang, X. Shen, Z. X. Shen, *Adv. Sci*., 2018, **5**, 1800621.

[S6] H. Xu, Y. Liu, Q. Bai, R. Wu, *J. Mater. Chem. A*, 2019, **7**, 3558-3562.

[S7] S. Liu, T. Zhao, X. Tan, L. Guo, J. Wu, X. Kang, H. Wang, L. Sun, W. Chu, *Nano Energy*, 2019, **63**, 103894.

[S8] S. Feng, J. Song, S. Fu, C. Zhu, Q. Shi, M. K. Song, D. Du, Y. Lin, *J. Mater. Chem. A,* 2017, **5**, 23737-23743.

[S9] W. Deng, X. Zhou, Q. Fang, Z. Liu, *J. Mater. Chem. A*, 2017, **5**, 13674-13682.

[S10] Y. Tan, Z. Zheng, S. Huang, Y. Wang, Z. Cui, J. Liu, X. Guo, *J. Mater. Chem. A*, 2017, **5**, 8360-8366.

[S11] H. Wu, L. Xia, J. Ren, Q. Zheng, C. Xu, D. Lin, *J. Mater. Chem. A*, 2017, **5**, 20458-20472.

[S12] Z. Li, Z. Xiao, S. Wang, Z. Cheng, P. Li, R. Wang, *Adv. Funct. Mater*., 2019, **29**, 1902322.